CHEMISTRY
AN ASIAN JOURNAL

DOI: 10.1002/asia.201100258

Molecular Triangles: Synthesis, Self-Assembly, and Blue Emission of Cyclo-7,10-tris-triphenylenyl Macrocycles

Matthias Georg Schwab,[a, b] Tianshi Qin,[a] Wojciech Pisula,[a] Alexey Mavrinskiy,[a] Xinliang Feng,[a] Martin Baumgarten,[a] Hun Kim,[a] Frédéric Laquai,[a] Sebastian Schuh,[c] Roman Trattnig,[c] Emil J. W. List,*[c, d] and Klaus Müllen*[a]

Abstract: A set of cyclo-7,10-tris-triphenylenyl macrocycles have been prepared by a Yamamoto cyclotrimerization protocol. In these novel macrocycles, three triphenylene units are covalently linked to each other, resulting in the formation of triangular-shaped molecules. The fully planar derivative revealed pronounced self-assembly behavior. NMR spectroscopy was used to determine the association constant in solution. 2D wide-angle X-ray scattering was applied to the study of the liquid crystallinity of this new discotic mesogen in the bulk state. Furthermore, nonplanar, laterally substituted derivatives were successfully tested as blue emitters in organic light-emitting diodes owing to their unique optoelectronic properties and their high stability. In this case, substitution with sterically demanding phenyl groups was efficiently used to suppress intermolecular packing, thus preventing undesired quenching effects.

Keywords: blue emission · liquid crystals · macrocycles · self-assembly · triphenylenes

Introduction

Triphenylene (TP) is a polycyclic aromatic hydrocarbon (PAH) that has been widely studied in chemistry and materials science owing to a manifold of fascinating properties. The triangular-shaped molecule owes its particular chemical stability to the fully benzenoid character of the aromatic system.[1,2] TP chemistry is well developed and various strategies for the buildup of substituted derivatives are available.[3,4] Monomeric TP derivatives received considerable interest when their liquid-crystalline nature was first reported,[5] spurring research in 2,3,6,7,10,11-hexasubstituted TP mesogens in particular.[6–11] Liquid crystallinity is driven by the strong π-stacking tendency of the planar TP core and van der Waals interactions of lateral side chains. Hexaalkoxytriphenylenes are of significant interest as fast photoconductors for applications in xerography.[9] In addition, polymers[12–15] and dendrimers[16–19] based on TP are also known to exhibit pronounced self-assembly behavior. A second major field of application is devoted to the optoelectronic properties of the molecule. TP is a famous blue emitter and has recently been investigated in organic optoelectronic devices.[13,15–17,20–22] Surprisingly, only a few macrocycles containing TP have been reported and so far little is known about the self-assembly of these cyclic systems in solution, on surfaces, and in the bulk state.[23–28] Moreover, the direct covalent linkage of three TP units within a macrocycle would raise the question to what degree the moderate luminescence yields of below 6% of monomeric TPs[29] can be boosted in a cyclic conjugated arrangement. It is hypothesized that this will enhance the transition dipole moment of the otherwise symmetry-forbidden $S_0 \rightarrow S_1$ transition.[30] This assumption is based on similar approaches, in which the symmetry in TP is broken by means of monofunctionalization using cyano substituents, leading to a threefold

[a] Dr. M. G. Schwab, Dr. T. Qin, Dr. W. Pisula, Dr. A. Mavrinskiy, Dr. X. Feng, Dr. M. Baumgarten, H. Kim, Dr. F. Laquai, Prof. Dr. K. Müllen
Max Planck Institute for Polymer Research
Ackermannweg 10,D-55128 Mainz (Germany)
Fax: (+49) 6131-379100
E-mail: muellen@mpip-mainz.mpg.de

[b] Dr. M. G. Schwab
BASF SE
Carl-Bosch-Straße 38, 67063 Ludwigshafen (Germany)

[c] S. Schuh, R. Trattnig, Prof. E. J. W. List
NanoTecCenter Weiz Forschungsgesellschaft mbH
Franz-Pichler-Straße 32, A-8160 Weiz (Austria)

[d] Prof. E. J. W. List
Institute of Solid State Physics
Graz University of Technology
Petersgasse 16, A-8010 Graz (Austria)
E-mail: e.list@tugraz.at

Supporting information for this article is available on the WWW under http://dx.doi.org/10.1002/asia.201100258.

increase in the luminescence yield,[31] or by symmetric methyl substitution, forcing the molecule to adopt a twisted conformation instead of a symmetric planar one.[32] Aryl–aryl cross-coupling macrocycles can be thought of as a toolbox. Frequently, macrocyclic systems are built up from two or more complementarily functionalized constituents following A_2B_2-type synthetic protocols, such as Suzuki–Miyaura or Sonogashira–Hagihara coupling reactions. However, AA-functionalized building units as well as BB-functionalized counterparts need to be synthesized prior to macrocycle formation.[33–36] In contrast, the cyclotrimerization of a single AA-functionalized precursor can significantly shorten the synthetic route and thereby enhance the overall yield. Examples of successful cyclotrimerization reactions involve the copper(II)-mediated reaction of Grignard reagents derived from biphenyl,[37] *ortho*-terphenyl,[38] and phenanthrene[39,40] and the trimerization of Lipshutz cuprates.[41] We have recently introduced the concept of a Yamamoto-based cyclotrimerization, which relied on the selective assembly of 3,6-dibromo-9,10-diarylphenanthrenes with halogen sites that included an ideal angle of 120°.[42,43]

Results and Discussion

Synthesis of Macrocycles

In this study, we extend the scope of suitable monomers to functional TPs successfully applied for the buildup of a set of triangular cyclo-7,10-tris-triphenylenyl macrocycles (**9**, **10a/10b**; Figure 1). Our motivation for the synthesis of these new cyclic trimers is twofold. A strong tendency to self-organize into stacked molecular aggregates can be anticipated from the flat dodecyloxy-substituted core of macrocycle **9**. Columnar mesophases adopted by discotic molecules in the bulk state have found great interest due to the possible application of such highly organized superstructures for charge transport in organic field-effect transistors (OFETs).[7,44–46] Whereas strong intermolecular packing was desired for macrocycle **9**, the two derivatives **10a/10b** were designed with respect to their use as fluorophores in organic light-emitting diodes (OLEDs). There, aggregation in the solid state is prevented to avoid self-quenching effects arising from intermolecular packing as well as bathochromic shifts in the emission spectrum due to excimer formation.[47,48] As such, the versatility of this design concept has been recently demonstrated for polymeric[13,14] and dendritic[16,17] materials containing TP units of identical topology. Hence, macrocycles **10a/10b** are characterized by shorter alkyl chains and additional twisted benzene units. Macrocycle **10a** contains six regularly distributed propyl chains, whereas a statistical hexyl substitution pattern is applied to **10b** to further suppress the aggregation of this derivative.

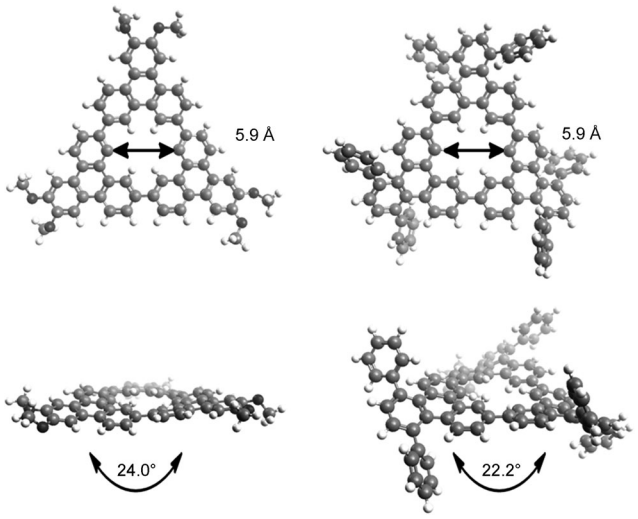

Figure 1. Conformation and geometric parameters of macrocycles **9** (left) and **10a/10b** (right), as derived from quantum chemical analysis (B3LYP, 6-311G*, side-chains are omitted).

In the first step, the preparation of the functionalized TP precursors **4**, **8a**, and **8b** was realized according to the two synthetic pathways depicted in Scheme 1. The functionalized and symmetrically substituted TP **4** was synthesized from 1,2-dibromo-4,5-bis(dodecyloxy)benzene (**1**)[49] by adopting a reported procedure for the analogous alkyl derivatives.[50] A double Suzuki–Miyaura coupling of **1** with phenyl boronic acid yielded the functionalized *ortho*-terphenyl **2**. The key step of this route consisted of building the TP backbone through the oxidative photocyclization of **2**, yielding 2,3-bis(dodecyloxy)triphenylene (**3**), which can be considered a model compound for the macrocycle itself, in 73%. The final bromination to yield 7,10-dibromo-2,3-bis(dodecyloxy)-triphenylene (**4**) was achieved by treatment of **3** with bromine in the presence of catalytic amounts of iron and iodine.

Regarding the synthesis of precursors **8a** and **8b**, another strategy had to be applied to realize phenyl substitution in the 1,4-position (Scheme 1). The point of departure was the bromination of phenanthrene-9,10-dione (**5**), according to a route established in the literature.[51] Subsequent Knoevenagel condensation of 3,6-dibromophenanthrene-9,10-dione (**6**) with diphenylacetone gave the functionalized phencyclone derivative **7**. In a final Diels–Alder [4+2] cycloaddition of **7** with oct-4-yne or oct-1-yne, the functionalized TPs **8a** (symmetric) and **8b** (asymmetric) were obtained, respectively, in high yields.

The cyclotrimerization reaction to yield the cyclo-7,10-tris-triphenylenyl macrocycles **9** and **10a/10b** was achieved by following standard Yamomoto conditions.[52,53] Hence, the catalyst was prepared under glovebox conditions, activated, and then the solution containing the TP precursor was added dropwise to guarantee pseudo-dilution conditions. Typically, the reaction was run at 60 (**9**) or 80°C (**10a/10b**) for 3 days in the dark. Quenching and decomposition of nickel residues was achieved by dropping the reaction mixture into a dilute solution of hydrochloric acid in methanol. The reaction products were isolated by using a combination of column chromatography on silica and recycling gel permeation chromatography (rGPC).

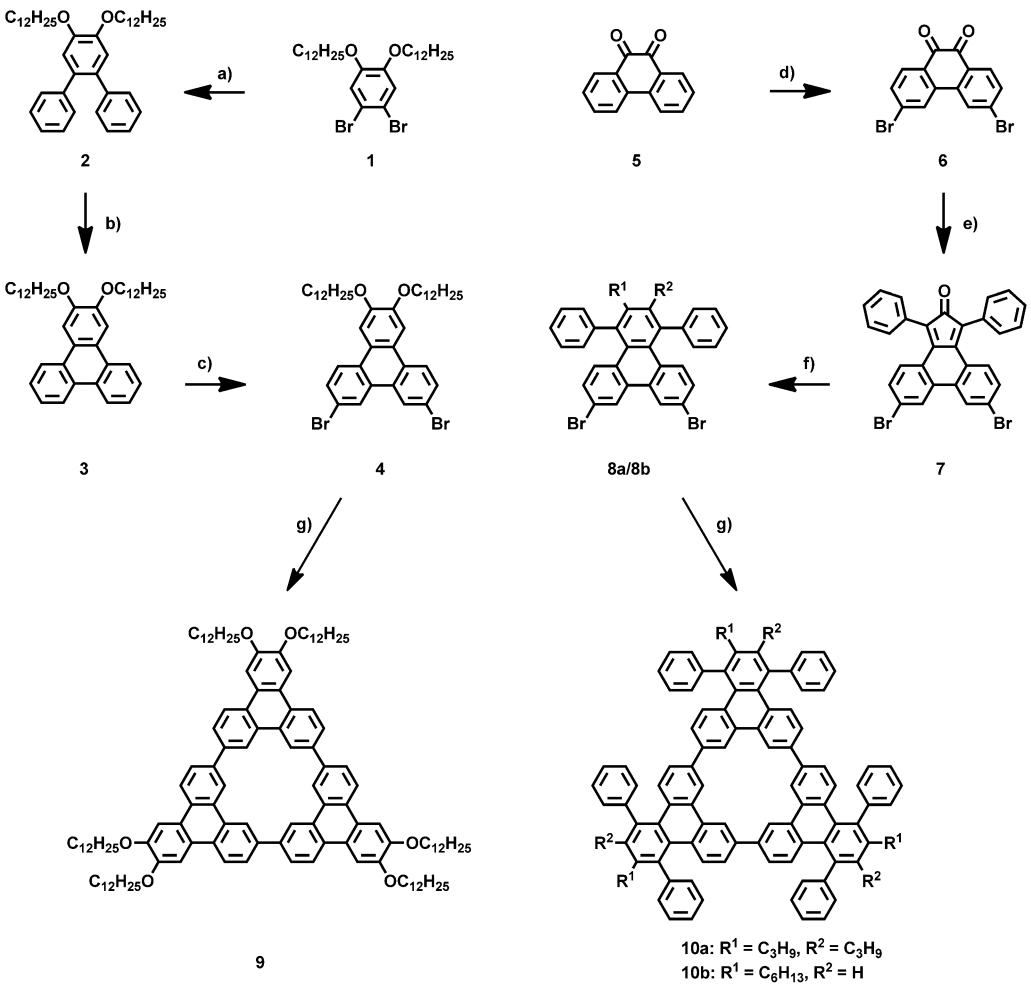

Scheme 1. Synthetic route to the macrocycles **9** and **10a/10b**, conditions: a) phenylboronic acid, $[Pd(PPh_3)_4]$, K_2CO_3, 1,4-dioxane, 100 °C, 87 %; b) *hv*, I_2, propylene oxide, toluene, RT, 73 %; c) Br_2, Fe/I_2, −5 °C, 66 %; d) *hv*, Br_2, nitrobenzene, 100 °C, 45 %; e) 1,3-diphenylpropan-2-one, KOH/MeOH, 80 °C, 74 %; f) **8a**: oct-4-yne, diphenyl ether, 220 °C, 81 %; **8b**: octy-1-ne, *ortho*-xylene, 170 °C, 92 %; g) **9**: $[Ni(cod)_2]$ (cod, = 2,2′-bipyridine), toluene/DMF, 60 °C, 21 %; **10a**: 80 °C, 70 %; **10b**: 80 °C, 77 %. DMF = *N*,*N*-dimethylformamide.

Quantum chemical calculations (B3LYP, 6-311G*) carried out on macrocycle **9** indicated a propeller-like structure with C_3 symmetry. As seen in the side-view representation in Figure 1, this manifests in a dihedral angle of 24.0° between two neighboring TP units. A cavity diameter of 5.9 Å was derived. Similar geometric parameters (22.2°, 5.9 Å) were found by computational analysis of the core of **10a/10b** (Figure 1). However, the aforementioned twisted arrangement of the lateral benzene rings is clearly visible and also induces a bent, nonplanar conformation of the three TP units.

Matrix-assisted laser desorption/ionization time-of-flight (MALDI-TOF) spectroscopy, after purification of **9** and **10a/10b**, indicated the successful construction of the macrocycles. In all cases, the signal of the target compound was exclusively observed (see the Supporting Information). The mass spectra recorded of the crude products revealed the presence of the de-halogenated monomer and dimer as major side products of the reaction. Further analysis of the macrocycles was carried out by means of ^1H and ^{13}C NMR spectroscopy. The spectra obtained were in agreement with the highly symmetric structure of **9** and **10a/10b** (see the Supporting Information). All three macrocycles displayed high solubility in common organic solvents.

Self-Assembly in Solution

The strong aggregation tendency of **9** became evident during handling and purification. Upon concentrating solutions of this macrocycle, turbidity appeared long before visible precipitation set in, indicating scattering effects from molecular aggregates. Furthermore, to suppress pronounced signal broadening, NMR spectroscopy analysis of **9** was performed at elevated temperatures in 1,1,2,2-tetrachloroethane ($[D_2]$TCE). Increasing the temperature resulted in a progressive downfield shift of the aromatic signals (see the Supporting Information). The strong temperature dependency seen in the ^1H NMR spectra motivated us to investigate the solution aggregation properties further. Temperature- and concentration-dependent NMR spectroscopy experiments

are known to be effective for the elucidation of the association constant, K_A, of disc-like aromatic systems in solution.[33,54,55]

The underlying theory is based on the observation that the chemical shift of a particular proton in a polymolecular stack is different from that of the single molecule. Thus, a dilution series from 8.0×10^{-3} to 7.0×10^{-5} M was performed in [D_2]TCE at 80 °C and the chemical shift of the protons indicating the macrocycle cavity was plotted as a function of concentration (Figure 2). A typical sigmoidal curve resulted, which was analyzed by using an attenuated K model according to a procedure described elsewhere.[33,54] From this model, a K_A value of 444 L mol^{-1} was calculated for the macrocycle **9**. This number is only slightly lower than that known for hexadodecyl-substituted hexa-*peri*-hexabenzocoronene (HBC) derivatives (457 L mol^{-1}),[55] highlighting strong π stacking for the cyclic TP trimer. Indeed, the number of benzene rings is 12 for macrocycle **9** and 13 for HBC, reflecting the similar size of the total π surface of both discs.

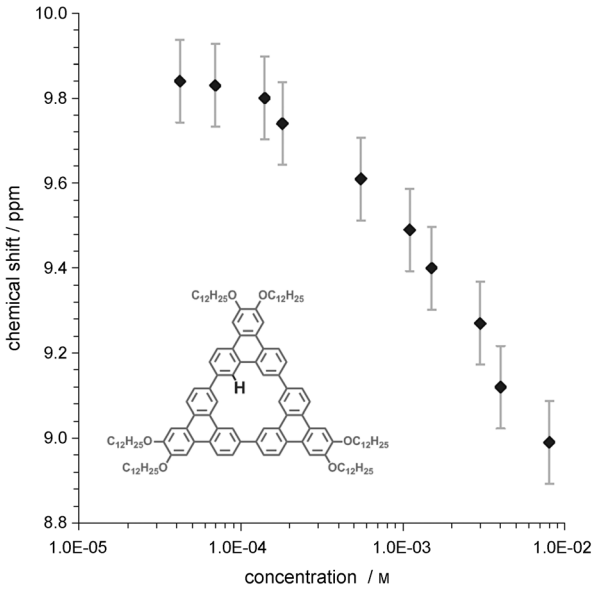

Figure 2. Concentration dependence of the ^{1}H NMR spectroscopy signal shift of macrocycle **9** in [D_2]TCE at 80 °C. TCE = 1,1,2,2-tetrachloroethane.

Liquid Crystallinity

Monomeric, alkyl-substituted TPs have also been widely studied in the field of discotic liquid crystals owing to the formation of mesophases that are generally characterized by a high degree of organization.[6,7,9–11] This structural perfection arises from the highly symmetric, disc-like aromatic core of TPs, which readily promotes their liquid crystallinity when decorated with peripheric alkyl chains. We were interested in the thermotropic behavior and the long-range self-assembly of the macrocyclic homologue **9**, which preserved several important features of TP-based liquid crystals. This refers in particular to the triangular shape reminiscent of TP itself and the positioning of six alkoxy substituents at the periphery of the molecule. Hence, the bulk-phase properties of macrocycle **9** were determined by two-dimensional wide-angle X-ray scattering (2D-WAXS) experiments and correlated to results from the thermal analysis by differential scanning calorimetry (DSC) (Figure 3).

The DSC trace showed two phase transitions that were fully reversible. Upon second heating, a minor endothermic peak was detected at T_{H1} = 64.3 °C and a second major endothermic transition occurred at T_{H2} = 109.1 °C. Both were found to reappear as exothermic transitions at T_{C1} = 55.5 °C and T_{C2} = 103.6 °C, respectively, when the sample was cooled down again (Figure 3A). 2D-WAXS measurements carried out on a mechanically extruded fiber of **9**[45] indicated that, above the phase transition temperature of 109.1 °C, a liquid-crystalline hexagonal columnar organization (Col_h) is adopted.[7] The equatorial reflections in the corresponding pattern (Figure 3B) revealed that the molecules pack in columnar structures, which assembled within a hexagonal unit cell defined by a parameter of a_{hex} = 3.55 nm. In the columns, the

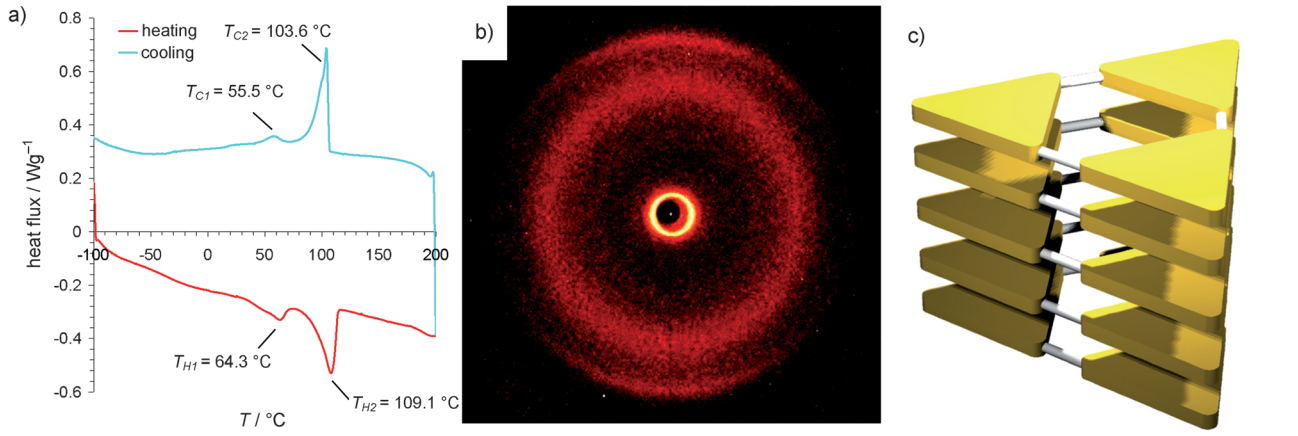

Figure 3. a) DSC trace of macrocycle **9** upon second heating (red) and cooling (blue); b) 2D-WAXS patterns of an extruded fiber of macrocycle **9** at 130 °C; c) schematic illustration of the proposed molecular packing of **9** in columnar structures, side-chains are omitted for clarity.

macrocycles stack on top of each other with a typical π-stacking distance of $p = 0.35$ nm.[44,45] The molecular plane is arranged orthogonal to the columnar axis, as depicted in the schematic illustration of Figure 3C. Characteristic for the liquid-crystalline phase, an amorphous halo appeared that could be attributed to the disordered dodecyloxy chains. Cooling the sample to 30 °C, this halo remained unaffected, while the columnar arrangement changed to a rectangular unit cell with $a_{rt} = 2.96$ nm and $b_{rt} = 2.03$ nm. When the temperatures of the phase transitions are compared to the thermotropic data of 2,3,6,7,10,11-hexakis(dodecyloxy)triphenylene,[11] an increased intermolecular packing can be deduced for macrocycle **9**. Hence, for the monomeric TP containing an identical number of six dodecyloxy chains, the transition to Col_h occurred at a much lower temperature of 55 °C and the clearing point was reached at 63 °C.[11] The significantly stronger aggregation of macrocycle **9** is not only evidenced by higher phase transition temperatures, but also by the fact that heating the compound to temperatures of 400–450 °C does not lead to isotropization of the sample and is ultimately limited by the thermal decomposition of the macrocycle. A comparably broad liquid-crystalline phase width has also been reported for a related cyclo-3,6-trisphenanthrenyl macrocycle.[42]

Optoelectronic Properties

We then investigated the optical and optoelectronic properties of macrocycles **9** and **10a/10b**, which strongly differed in the degree of planarity and symmetry, as seen in Figure 1. To characterize the basic optical properties and study the aggregation behavior, macrocycles **9** and **10a/10b** were investigated in solution (Figure 4) and as thin films (Figure 6, see below) with respect to their photoluminescence (PL) emission, PL quantum yield (PLQY), and absorption properties. All relevant values are summarized in Table 1.

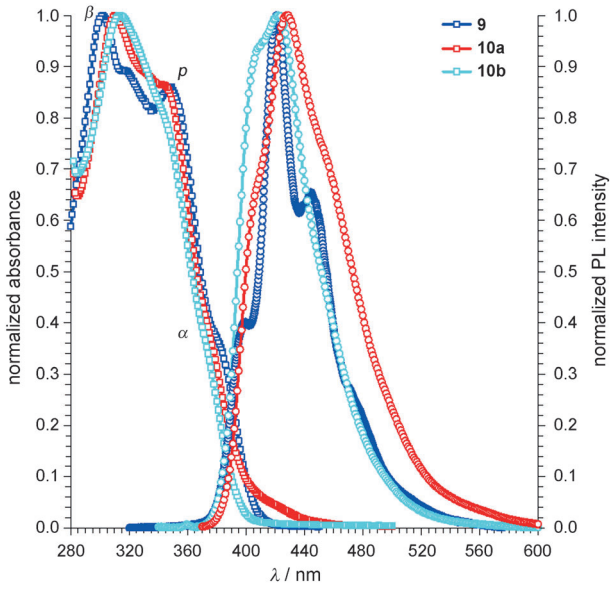

Figure 4. Normalized UV/Vis absorption spectra and normalized PL emission spectra of macrocycles **9**, **10a**, and **10b** in toluene (1.1×10^{-4} M).

In general, according to Clar, the bands in the absorption spectra of PAHs can be classified as α, β, and p bands.[1,2] As for parent TP,[56] these characteristic bands manifest in the absorption spectrum of all macrocycles and appear at similar wavelengths owing to the common aromatic structure of the cyclic backbone (Figure 4). For instance, the bands are located at $\lambda_\beta = 302$, $\lambda_p = 346$, and $\lambda_\alpha = 386$ nm in the case of **9**. The high degree of vibronic fine structure is also mirrored in the corresponding PL emission spectra depicted in Figure 4 for solution measurements. The corresponding maximum values, λ_{em}, are found at 421 (**9**), 422 (**10a**), and 430 nm (**10b**). With respect to monomeric TP with its emission maximum located at 376 nm,[56] as well as 1,2,4-triphenyltriphenylene (TPTP) with an emission maximum at 401 nm,[16] the observed bathochromic shift of the three macrocycles can be clearly attributed to the cyclic conjugated arrangement.

Table 1. Summary of relevant optical properties for **9**, **10a**, and **10b** as determined in toluene (1.1×10^{-4} M). The previously reported data for parent TP and TPTP is given for comparison.

	In solution		Thin films	
	$\lambda_{em\ (max)}$ [nm]	Φ_{PL}[a] [%]	$\lambda_{em\ (max)}$ [nm]	Φ_{PL}[b] [%]
TP[c]	376	6	–	–
TPTP[d]	401	5	402	–
9	421	64	479	< 1
10a	422	68	480	13
10b	430	38	425	43

[a] Taking quinine sulfate dehydrate as a standard reference. [b] Taking poly(fluorene) as a standard reference. [c] Data taken from reference [56]. [d] TPTP = 1,2,4-triphenyltriphenylene; data taken from reference [16].

All three compounds exhibit an intense blue PL that is located close to the ideal value for blue-emitting OLEDs.[13,15–17,20–22] Comparing the limited PLQY, Φ_{PL}, of 6.0% for parent TP[29] and only 5.0% for TPTP (a phenyl-substituted, twisted, non-planar TP)[16] to those of **9** and **10a/10b**, up to a tenfold improvement in the PLQY for the macrocyclic arrangement can be observed. Macrocycles **9** and **10a** exhibit a PLQY of 64 and 68%, respectively, whereas for **10b** a PLQY of 38% was determined. This result clearly confirms the original hypothesis for this work and the aim to increase the transition dipole moment of the otherwise symmetry-forbidden $S_0 \rightarrow S_1$ transition through a cyclic conjugated arrangement.[30] By this reasoning, the PLQY of the TP unit is greatly enhanced, while the transition energy (emission maximum) is only slightly changed from the near UV to the center of the blue region of the spectrum. Similar to other systems, the oscillator strength of the emissive transition is enhanced by the macrocycle approach because the overall symmetry of the TP unit is effectively broken (Figure 1).[31] Moreover, this new molecular design forces the TPs to adopt a contorted instead of a fully planar conformation, which further influences the transition dipole of the molecule.[32] In addition, the overall increased

transition dipole, and thereby, enhanced radiative decay rate should also make the impact of intersystem crossing to the triplet manifold on the total excited-state lifetime less dominant, as examined in the following discussion.

Regarding the nature of the excited states of single fluorophores and aggregates in solution, important information can be derived from time-resolved PL measurements, as recently exemplified by a series of oligothiophenes.[57] In combination to the analysis carried out by means of ^{1}H NMR spectroscopy (Figure 2), the pronounced solution aggregation behavior of **9** was thus studied in more detail and also compared with that of the monomeric model compound 2,3-bis(dodecyloxy)triphenylene (**3**). The measurements were performed in toluene at a concentration of 1.1×10^{-4} M, thus at a concentration at which mainly the fluorescence of isolated molecules can be expected with a small contribution from aggregates. Figure 5A shows a comparison of time-resolved PL spectra of **9** at different delay times after excitation and Figure 5B depicts a fluorescence decay transient of **9** fitted to a biexponential decay pattern. These results were derived from streak camera experiments by using femtosecond laser pulse excitation.

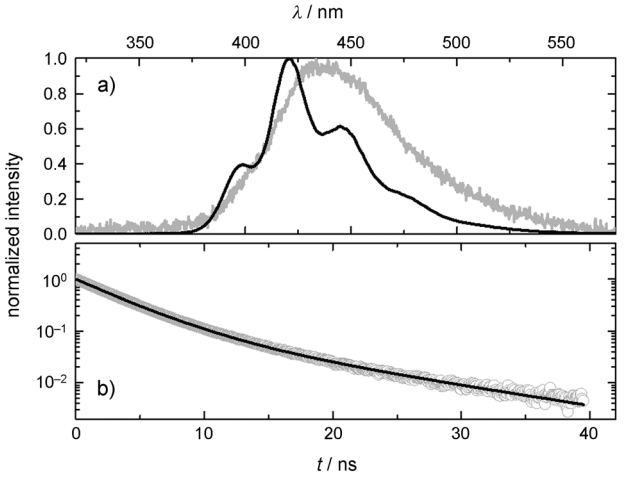

Figure 5. a) Normalized time-resolved PL spectra of **9** immediately after excitation (black) and at a delay of 21 ns (gray) in toluene at a concentration of 1.1×10^{-4} M. b) PL decay transient (gray circles) of **9** and biexponential fit (black) to the data with decay times of $\tau_1=3.7$ ns and $\tau_2=11.2$ ns.

The spectrum straight after excitation exhibits virtually the same vibronic features as the steady-state measurements shown in Figure 4a with a maximum λ_{em} at 421 nm and vibronic replica at 395 and 445 nm. However, after 21 ns, the spectrum has evolved into a broad and featureless emission with the maximum redshifted by 11 nm with respect to the early spectrum, now centered at 433 nm. Clearly, a second fluorescent species is present at this concentration; however, its longer lifetime and less-efficient emission allow observation only after the intense fluorescence of the isolated species has decayed. The second broad and longer-lived component of the spectrum is a consequence of the high tendency of macrocycle **9** to aggregate, even in dilute solutions at concentrations as low as 1.1×10^{-4} M.

Also, the fluorescence decay transient of **9** is indicative of a second contribution to the overall emissive behavior. In fact, two different decay channels are identified, since the decay transient can be sufficiently well described by a sum of two exponentials, similar to previously reported results on TP liquid crystals and dendrimers (Figure 5B).[8,19] The first component has a lifetime of $\tau_1=3.7$ ns and an amplitude of 0.87, whereas the second component is characterized by $\tau_2=11.2$ ns and an amplitude of 0.13. The former can be ascribed to the fluorescence of the individual macrocycles, whereas the latter arises from aggregated species. This assignment was further supported by experiments at higher and lower analyte concentrations, since the amplitude of the shorter-lived component was found to increase upon dilution and to decrease at higher concentration, thus reflecting the impact of aggregation. The broad and featureless, as well as slightly redshifted, spectrum further supports the assignment of the emission as fluorescence from aggregates present in solution.

Finally, a closer comparison of the fluorescence lifetimes of macrocycle **9** with model compound **3** by time-resolved PL spectroscopy revealed that the fluorescence lifetime reduced from 10.0 ns for **3** (see the Supporting Information) to 3.7 ns, as obtained from the fits depicted above. This strongly supports the previous conclusion of stronger electronic coupling of the lowest π–π* singlet excited state to the ground state in the cyclic trimer than in model compound **3**.

Device Results

The solid-state PL spectra obtained by measurements of thin films prepared by spin-coating indicated significant differences for the three macrocycles (Figure 6). As clearly observed for **9** and **10a**, the PL emission maximum undergoes a dramatic bathochromic shift from about 420 to 480 nm. The shift of the PL maximum is accompanied by a severe broadening of the emission spectrum, a loss of the vibronic structure, and a significant decrease in PLQY in the solid state (Table 1). All three observations are a clear indication of aggregation in the bulk state and excimer formation due to intermolecular packing.[47,48] On the contrary, macrocycle **10b**, containing three statistically arranged hexyl side chains, does not show this strong alteration of the emission spectrum upon changing from solution to the solid state. Here only a very moderate redshift of 5 nm is observed for the emission maximum, no loss of the vibronic features is found, and no significant quenching of the PLQY in the solid state is observed. Macrocycle **10b** exhibits a PLQY that is about 40% of that of poly(fluorene) (PF)—a blue emitting polymer with a similar emission spectrum and a state-of-the-art PLQY and documented good OLED performance.

CHEMISTRY
AN ASIAN JOURNAL

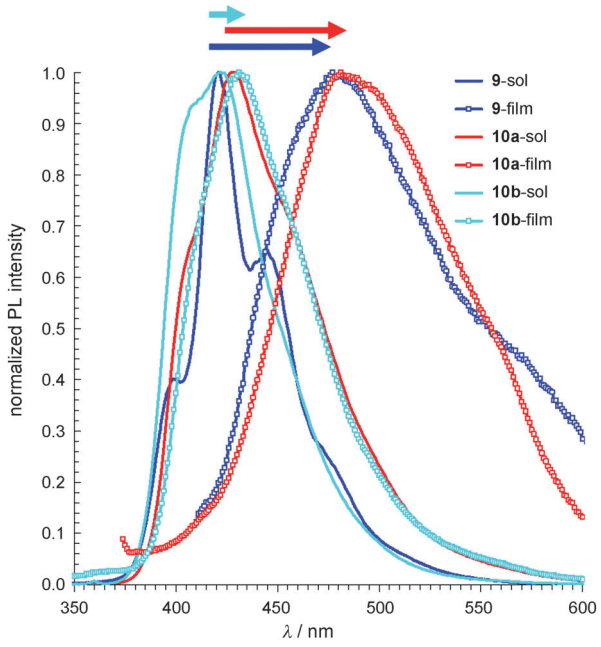

Figure 6. Comparison of a normalized solution (1.1×10^{-4} M) in toluene and solid-state PL emission spectra of **9**, **10a**, and **10b** obtained from spin-coated thin films.

Therefore, macrocycle **10b** was chosen as an active blue emitter in a simple two-layer, solution-processed OLED configuration with 1,3,5-tri(1-phenyl-1*H*-benzo[*d*]imidazol-2-yl)phenyl (TPBi) as an electron-transport layer in a indium tin oxide (ITO)/poly(3,4-ethylenedioxythiophene)–poly(styrenesulfonate) (PEDOT:PSS)/**10b**(50 nm)/TPBi(10 nm)/Ca-(10 nm)/Al device.[17] The results are depicted in Figure 7.

The electroluminescence (EL) onset for the device is observed at 3.9 V. The maximum luminance is found to be 200 cd m^{-12} at 6.5 V; macrocycle **10b** shows a narrow deep-blue emission similar to PL with Commission Internationale De L'Eclairage (CIE) $(xy)=(0.16, 0.07)$. All devices fabricated from **10b** showed good stability over time and no aggregation effects and related changes in the emission spectrum were observed when keeping the current densities in the device below 2500 A m^{-12}. When driving the device above this current density value, a redshift of the emission was observed. This was attributed to a thermally induced reorganization of the active layer as a consequence of the Joule heating during operation of the device. It can be supposed that the increased molecular mobility at higher temperature results in an undesired cofacial orientation of the molecular cores despite the bulkiness of the lateral substituents. For comparison, macrocycle **10a** was also tested in EL devices (not shown) and the device exhibited a green-emission EL spectra similar to those observed in PL with a maximum of 600 cd m^{-12} at 6.5 V and CIE $(xy)=(0.20, 0.31)$. The experiments carried out on the TP macrocycles demonstrated the great potential of this new class of blue emitters for solution-processed, small-molecule OLED applications. Benchmarking the attained performance against results obtained for devices based on polymers[12–15] and dendrimers[16–19] using TP building blocks clearly revealed that the cyclic TP trimers exhibited a strongly improved PLQY; an essential parameter of high-performance OLEDs. However, the materials need to be further improved in terms of thermal stability to avoid reorganization/recrystallization before further device optimization work can take place.

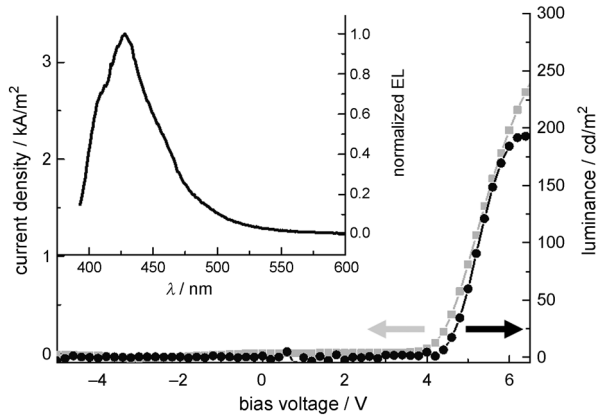

Figure 7. Voltage/current (gray) and voltage/luminance (black) characteristics of ITO/PEDOT:PSS/**10b** (50 nm)/TPBi (10 nm)/Ca (10 nm)/Al diode; the inset shows the corresponding EL spectrum of **10b**.

Conclusion

Three new cyclo-7,10-tris-triphenylenyl macrocycles were successfully prepared by using a Yamamoto-type cyclotrimerization approach. This flexible synthetic protocol allowed for the buildup of molecular triangles in which the TP units were directly linked to each other. By introducing long alkoxy side chains to the core of the macrocycle, strong self-assembly can be induced that is in analogy to the properties of monomeric alkyl-substituted TPs. As such, a high association constant, K_A, that was of the same order of magnitude as those of HBC derivatives could be derived from NMR spectroscopy solution experiments. The liquid crystallinity of the discotic molecule was studied by means of 2D-WAXS and correlated to its thermal properties. The highly organized columnar superstructures adopted by this fully planarized macrocycle could be applied as charge-carrier pathways in OFET devices. The comparative study of the optical properties of the three cyclic trimers revealed significant differences that could be correlated to the nature of the peripheral groups and their substitution pattern. On the one hand, all three compounds showed deep-blue emission in solution and a tenfold increase in the PLQYs with respect to parent TP as a result of conjugation along the cyclic backbone, which strongly increased the transition dipole moment of the otherwise symmetry-forbidden $S_0\rightarrow S_1$ transition. On the other hand, the intrinsic intermolecular packing tendency could only be sufficiently disrupted to confine the favorable PL properties to the solid state for one derivative that was composed of two regioisomers. The macrocycle was tested successfully as an active component in the emissive

layer of an OLED and showed promising performance both regarding emissive properties and device stability. However, for future studies, even more bulky side groups should be attached to the TP moieties to further suppress the observed thermal reassembly at a high driving current if OLED applications of the macrocycles are envisaged.

Experimental Section

Techniques

^{1}H and ^{13}C NMR spectra were recorded on Bruker DPX250 and DRX500 spectrometers, respectively, and referenced to residual signals of the deuterated solvent. Field-desorption mass spectra (FD/MS) were performed with a VG Instruments ZAB 2-SE-FDP spectrometer using 8 kV accelerating voltage. MALDI-TOF mass spectra were measured by using a Bruker Reflex II instrument utilizing a 337 nm nitrogen laser, calibrated against poly(ethylene glycol) (3000 g mol^{-1}). The 2D-WAXS experiments of orientated filaments were performed by means of a rotating anode (Rigaku 18 kW) X-ray beam with a pinhole collimation and a 2D Siemens detector with a beam diameter of 1.0 mm. A double graphite monochromator for the $Cu_{K\alpha}$ radiation ($\lambda = 0.154$ nm) was used. The patterns were recorded with vertical orientation of the filament axis and with the beam perpendicular to the filament.

For time-resolved PL spectroscopy, the materials were dissolved in toluene at a concentration of 0.2 mg mL^{-1} and the solutions were transferred into quartz glass cuvettes with a thickness of 1 mm. The samples were excited at 300 nm with the output of a commercial laser system consisting of an optical parametric amplifier (Coherent OPerA Solo) itself pumped by the output of a titanium:sapphire femtosecond amplifier (Coherent LIBRA HE) operating at a repetition rate of 1 kHz with a pulse width of 100 fs. The emitted light was collected by an optical telescope and focused into a spectrograph for spectral dispersion and detected by a C4742 Hamamatsu Streak Camera system.

For the OLED devices, ITO-covered glass substrates were cleaned with acetone, toluene, and isopropanol and subsequently exposed to oxygen plasma. PEDOT:PSS layers were spin-coated under ambient conditions and dried under an inert atmosphere. Subsequently, the active material dissolved in toluene (5.0 g L^{-1}) was spin-coated on top of the PEDOT:PSS layer, resulting in a film thickness of about 50 nm, which was dried at 120 °C under a dynamic vacuum less than 1×10^{-5} mbar. The multilayer cathode and TPBi was thermally deposited in a vacuum coating unit at base pressures less than 3×10^{-6} mbar. The luminescence/voltage measurements were performed by using an integrating sphere equipped with a silicon photodiode and a computer controlled Keithley 237 source measurement unit. Spectral characterization was done with a Lot-Oriel Multispec equipped with a DB 401-UV CCD camera from Andor. The quantum chemical calculations were performed by the DFT approach with B3LYP hybrid functionals using the 6-31G* basis set.[58]

Materials

1,2-Dibromo-4,5-bis(dodecyloxy)benzene (**1**)[49] and 3,6-dibromophenanthrene-9,10-dione (**6**)[51] were synthesized according to the literature procedures. All other chemicals and solvents were purchased from commercial sources and used without further purification. Solvents for synthesis were purified according to standard procedures. Reactions were carried out under an argon atmosphere.

*Synthesis of **2***

1,2-Dibromo-4,5-bis(dodecyloxy)benzene (**1**, 6.00 g, 9.92 mmol) and phenylboronic acid (3.63 g, 29.77 mmol) were dissolved in toluene (150.0 mL). Then, a 2 M aqueous solution of potassium carbonate (40.0 mL) and a few drops of Aliquat 336 were added. After degassing by argon bubbling, tetrakis(triphenylphosphine)palladium(0) (2.29 g, 1.98 mmol) were added and the resulting mixture was heated to reflux for 24 h. The precipitate that was formed during the reaction was collected by filtration, washed with methanol, and used for the next step without further purification. Compound **2** was obtained as a white solid (5.17 g, 8.63 mmol, 87 %). ^{1}H NMR (300 MHz, CD_2Cl_2): $\delta = 7.24$–7.08 (m, 10 H), 6.93 (s, 2 H), 4.04 (t, $J = 6.6$, 4 H), 1.82 (p, 4 H), 1.56–1.18 (m, 36 H), 0.88 ppm (t, $J = 6.7$, 6 H); ^{13}C NMR (75 MHz, CD_2Cl_2): $\delta = 149.08$, 142.32, 133.75, 130.57, 128.36, 126.71, 116.94, 70.11, 32.56, 30.33, 30.27, 30.05, 29.99, 26.69, 23.31, 14.49 ppm; MS (FD, 8 kV): m/z (%): 595.0 (100.0) [M^+].

*Synthesis of **3***

Compound **2** (0.50 g, 0.83 mmol) and iodine (0.23 g, 0.91 mmol) were dissolved in toluene (120.0 mL). Then propylene oxide (0.4 mL, 5.72 mmol) was added. The solution was irradiated with 300 nm (40 W) for 48 h at room temperature. The crude product was purified by column chromatography (hexane/ethyl acetate = 20/1) to yield **3** as a white solid (0.36 g, 0.61 mmol, 73 %). ^{1}H NMR (300 MHz, CD_2Cl_2): $\delta = 8.66$ (d, $J = 8.6$, 2 H), 8.52 (d, $J = 8.7$, 2 H), 8.03 (s, 2 H), 7.70–7.57 (m, 4 H), 4.24 (t, $J = 6.6$, 4 H), 1.93 (p, 4 H), 1.65–1.18 (m, 36 H), 0.88 ppm (t, $J = 6.6$, 6 H); ^{13}C NMR (75 MHz, CD_2Cl_2): $\delta = 150.3$, 130.1, 129.6, 127.6, 126.8, 124.7, 123.9, 123.4, 107.3, 69.9, 32.5, 30.7, 30.3, 30.3, 30.1, 30.0, 26.7, 23.3, 14.5 ppm; MS (FD, 8 kV): m/z (%): 593.5 (100.0) [M^+]; elemental analysis calcd (%) for $C_{42}H_{62}O_2$: C 84.51, H 10.13; found: C 87.21, H 10.98.

*Synthesis of **4***

Compound **3** (1.00 g, 1.68 mmol) was dissolved in CH_2Cl_2 (18.0 mL) and a catalytic amount of iron powder and iodine was added. Then, a solution of bromine (1.08 g, 6.76 mmol) in CH_2Cl_2 (7.2 mL) was added dropwise at a temperature of −5 °C. The reaction was allowed to proceed at this temperature for 3 h after what it was stopped by the addition of a 10 % solution of sodium thiosulfate. The crude product was recrystallized from CH_2Cl_2 to yield **4** as a white crystalline solid (0.84 g, 1.11 mmol, 66 %). ^{1}H NMR (300 MHz, THF): $\delta = 8.83$ (s, 2 H), 8.50 (d, $J = 8.8$, 2 H), 8.03 (s, 2 H), 7.73 (d, $J = 8.7$, 2 H), 4.23 (t, $J = 6.1$, 4 H), 1.89 (p, 4 H), 1.43 (m, 36 H), 0.89 ppm (t, $J = 6.6$, 6 H); ^{13}C NMR (75 MHz, THF): $\delta = 151.7$, 131.5, 130.9, 130.2, 127.3, 126.1, 124.8, 121.5, 107.7, 70.0, 33.1, 30.9, 30.9, 30.8, 30.6, 30.5, 27.3, 23.7, 14.6 ppm; MS (FD, 8 kV): m/z (%): 754.2 (100.0) [M^+]; elemental analysis calcd (%) for $C_{42}H_{60}O_2Br_2$: C 66.84, H 7.75; found: C 64.19, H 5.12.

*Synthesis of **7***

3,6-Dibromophenanthrene-9,10-dione (**6**; 0.88 g, 2.40 mmol) and 1,3-diphenyl-2-propanone (0.75 g, 3.57 mmol) were dissolved in anhydrous MeOH (50.0 mL) under an argon atmosphere. Then, a solution of KOH (0.15 mL) in MeOH (2 M) was added dropwise and the mixture was heated to 80 °C for 5 min. The brown mixture was fast frozen to 0 °C and HCl (1.9 mL; 1.25 M in MeOH) was added with stirring to neutralize the solution to pH 5. The green precipitate was filtered off, washed with cold MeOH, and purified by column chromatography (hexane/CH_2Cl_2 = 2/1), affording **7** as a dark green powder (0.95 g, 1.75 mmol, 74 %). ^{1}H NMR (250 MHz, CD_2Cl_2): $\delta = 7.93$ (d, $J = 1.9$ Hz, 2 H), 7.43 (dd, $J = 7.4$, 5.5 Hz, 6 H), 7.39–7.29 (m, 6 H), 7.11 ppm (dd, $J = 8.6$, 1.9 Hz, 2 H). ^{13}C NMR (62.5 MHz, CD_2Cl_2): $\delta = 197.8$, 147.4, 137.8, 136.2, 134.4, 133.0, 132.6, 132.1, 130.2, 129.0, 128.7, 128.6, 128.2, 127.1, 126.7, 124.2, 123.8, 106.8 ppm. MS (FD, 8 kV): m/z (%): 540.2 (100.0) [M^+].

*Synthesis of **8a***

6,9-Dibromophencyclone (**7**; 450 mg, 0.83 mmol) and oct-4-yne (183 mg, 1.66 mmol) were dissolved in diphenyl ether (10.0 mL) in a microwave tube. The argon-bubbled mixture was stirred at 220 °C under 300 W microwave irradiation for 8 h. After cooling to room temperature, the reaction mixture was precipitated into MeOH, and further purified by column chromatography (hexane/CH_2Cl_2 = 4/1), affording **8a** (418 mg, 0.67 mmol, 81 %). ^{1}H NMR (300 MHz, CD_2Cl_2): $\delta = 8.43$ (d, $J = 2.1$ Hz, 2 H), 7.53–7.39 (m, 8 H), 7.33 (dd, $J = 7.3$, 2.0 Hz, 4 H), 7.10 (dd, $J = 9.1$, 2.1 Hz, 2 H), 2.90–2.73 (m, 4 H), 1.37–1.16 (m, 4 H), 0.70 ppm (t, $J = 7.3$ Hz, 6 H). ^{13}C NMR (75 MHz, CD_2Cl_2): $\delta = 143.3$, 140.6, 138.5, 132.2, 131.5, 130.5, 129.4, 129.1, 129.1, 127.5, 126.1, 120.4, 115.4, 32.8, 24.8,

14.5 ppm; MS (FD, 8 kV): *m/z* (%): 622.2 (100.0) [M^+]; elemental analysis calcd (%) for $C_{36}H_{30}Br_2$: C 69.47, H 4.86; found: C 69.53, H 4.80.

Synthesis of ***8b***

6,9-Dibromophencyclone (**7**; 450 mg, 0.83 mmol) and 1-octyne (183 mg, 1.66 mmol) were dissolved in *ortho*-xylene (10.0 mL) in a microwave tube. The argon bubbled mixture was stirred at 170 °C under 300 W microwave irradiation for 8 h. After cooling to room temperature, the reaction mixture was precipitated into MeOH and further purified by column chromatography (hexane/CH_2Cl_2 = 4:1), affording **8b** (475 mg, 0.76 mmol, 92%). ^{1}H NMR (300 MHz, CD_2Cl_2): δ = 8.48 (t, J = 2.4 Hz, 2H), 7.55 (t, J = 4.5 Hz, 2H), 7.51–7.38 (m, 9H), 7.30 (dd, J = 7.4, 2.0 Hz, 2H), 7.15 (ddd, J = 15.6, 9.0, 2.0 Hz, 2H), 2.77–2.58 (m, 2H), 1.52 (s, 2H), 1.18 (d, J = 7.4 Hz, 6H), 0.82 ppm (t, J = 6.8 Hz, 3H). ^{13}C NMR (75 MHz, CD_2Cl_2): δ = 144.6, 142.3, 141.4, 138.9, 132.8, 132.5, 131.8, 131.7, 131.4, 129.8, 129.6, 129.4, 129.3, 129.1, 127.73, 127.65, 126.2, 120.9, 33.8, 31.8, 31.6, 29.6, 22.9, 14.2 ppm; MS (FD, 8 kV): *m/z* (%): 622.2 (100.0) [M^+]; elemental analysis calcd (%) for $C_{36}H_{30}Br_2$: C 69.47, H 4.86; found: C 69.51, H 4.72.

Synthesis of ***9***

The catalyst solution was prepared inside the glovebox by adding DMF (6.0 mL) and toluene (12.0 mL) to a mixture of bis(cyclooctadiene)nickel(0) (0.12 g, 0.47 mmol), 2,2′-bipyridine (0.07 g, 0.47 mmol) and cyclooctadiene (0.05 mL, 0.47 mmol). The resulting solution was stirred for 30 min at 60 °C. Then, a solution of **4** (0.15 g, 0.20 mmol) in toluene (4.0 mL) was added dropwise over 30 min. The reaction mixture was stirred for 12 h at 60 °C under the exclusion of light. After cooling, the mixture was diluted with diethyl ether and washed with diluted hydrochloric acid (2 M). The crude product was prepurified by column chromatography on silica gel (CH_2Cl_2/methanol = 10/1). Further purification was achieved by preparative gel permeation chromatography (chloroform) to yield **9** as a white solid (25 mg, 0.014 mmol, 21%). ^{1}H NMR (300 MHz, $CDCl_3$): δ = 7.95 (s, 6H), 7.35 (d, J = 7.6, 6H), 7.16 (d, J = 8.1, 6H), 7.03 (s, 6H), 3.75 (t, J = 4.1, 12H), 1.79 (p, 12H), 1.55–1.28 (m, 108H), 0.91 ppm (t, J = 6.7, 18H); ^{13}C NMR (75 MHz, $CDCl_3$): δ = 148.3, 133.2, 128.2, 128.0, 123.2, 122.1, 121.9, 117.7, 105.4, 68.4, 31.8, 29.7, 29.6, 29.33, 29.29, 26.1, 22.5, 13.9 ppm; MS (MALDI-TOF): *m/z* (%): 1783.39 (100.0) [M^+].

Synthesis of ***10a***

Bis(cyclooctadiene)nickel(0) (286 mg, 1.04 mmol), cyclooctadiene (0.13 mL, 1.04 mmol), and 2,2′-bipyridine (162 mg, 1.04 mmol) were dissolved in dry toluene (1.0 mL) and dry DMF (2.0 mL) in a Schlenk tube under glovebox conditions. The resulting solution was stirred for 20 min at 60 °C and then a solution of **8a** (270 mg, 0.43 mmol) in dry toluene (12.0 mL) was added dropwise over 30 min. The reaction mixture was stirred for 12 h at 80 °C under the exclusion of light. After cooling to room temperature, the reaction mixture was precipitated into MeOH, and further purified by column chromatography (hexane/CH_2Cl_2 = 3/1), affording **10a** (142 mg, 0.10 mmol, 70%). ^{1}H NMR (300 MHz, CD_2Cl_2): δ = 9.35 (s, 6H), 8.53 (s, 6H), 7.54 (s, 6H), 7.47–7.29 (m, 30H) 2.79 (s, 12H), 1.37–1.16 (m, 12H), 0.70 ppm (t, J = 7.3 Hz, 18H); ^{13}C NMR (125 MHz, THF): δ = 143.9, 139.2, 138.6, 135.5, 135.3, 131.9, 131.6, 129.5, 128.5, 126.8, 122.5, 119.9, 119.7, 32.5, 29.7, 13.7 ppm; MS (MALDI-TOF): *m/z* (%): 1387.14 (100.0) [M^+]; elemental analysis calcd (%) for $C_{108}H_{90}$: C 93.46, H 6.54; found: C 93.50, H 6.47.

Synthesis of ***10b***

Same procedure as that used for **10a**, yielding **10b** as a solid (153 mg, 0.11 mmol, 77%). The final product contained two inseparable isomers (1,1′,1″ and 1,1′,2″ hexyl-substituted). ^{1}H NMR (300 MHz, CD_2Cl_2): δ = 9.46 (s, 6H), 8.70–8.28 (m, 6H), 7.70–7.59 (m, 6H), 7.53–7.23 (m, 33H), 2.83–2.60 (m, 6H), 1.63–1.10 (m, 24H), 0.80 ppm (t, J = 6.8 Hz, 9H); ^{13}C NMR (125 MHz, THF): δ = 142.6, 139.8, 139.0, 138.5, 138.4, 137.4, 131.7, 131.6, 131.0, 130.9, 130.1, 129.4, 128.8, 126.8, 124.5, 124.38, 124.36, 122.4, 121.8, 33.4, 31.4, 29.2, 22.4, 13.4 ppm; MS (MALDI-TOF): *m/z* (%): 1387.33 (100.0) [M^+]; elemental analysis calcd (%): C 93.46, H 6.54; found: C 93.48, H 6.49.

Acknowledgements

M.G.S. thanks the "Graduate School Materials Science in Mainz" for a scholarship. H.K. acknowledges funding from the IRTG1404: Self-organized materials for optoelectronics provided by the DFG. F.L. thanks the Max Planck Society for funding of a Max Planck Research Group. R.T. thanks the BMWFJ and the Christian Doppler Society for the financial support. We would like to thank Lei Dou for the computational analysis of the NMR spectroscopy data.

[1] E. Clar, *The Aromatic Sextet*, Wiley, London, **1972**.
[2] R. Rieger, K. Müllen, *J. Phys. Org. Chem.* **2010**, *23*, 315.
[3] C. M. Buess, D. D. Lawson, *Chem. Rev.* **1960**, *60*, 313.
[4] D. Pérez, E. Guitián, *Chem. Soc. Rev.* **2004**, *33*, 274.
[5] J. Billard, J. C. Dubois, N. H. Tinh, A. Zann, *Nouv. J. Chimie* **1978**, *2*, 535.
[6] S. Kumar, *Liq. Cryst.* **2004**, *31*, 1037.
[7] S. Laschat, A. Baro, N. Steinke, F. Giesselmann, C. Hägele, G. Scalia, R. Judele, E. Kapatsina, S. Sauer, A. Schreivogel, *Angew. Chem.* **2007**, *119*, 4916; *Angew. Chem. Int. Ed.* **2007**, *46*, 4832.
[8] D. Markovitsi, I. Lécuyer, P. Lianos, J. Malthête, *J. Chem. Soc. Faraday Trans.* **1991**, *87*, 1785.
[9] D. Adam, P. Schuhmacher, J. Simmerer, L. Häussling, K. Siemensmeyer, K. H. Etzbachi, H. Ringsdorf, D. Haarer, *Nature* **1994**, 141.
[10] P. Henderson, S. Kumar, J. A. Rego, H. Ringsdorf, P. Schuhmacher, *J. Chem. Soc. Chem. Commun.* **1995**, 1059.
[11] O. V. Zemtsova, K. N. Zheleznov, *Russ. Chem. Bull.* **2004**, *53*, 1743.
[12] S. Kumar, *Liq. Cryst.* **2005**, *32*, 1089.
[13] M. Saleh, Y. S. Park, M. Baumgarten, J. J. Kim, K. Müllen, *Macromol. Rapid Commun.* **2009**, *30*, 1279.
[14] M. Saleh, M. Baumgarten, A. Mavrinskiy, T. Schäfer, K. Müllen, *Macromolecules* **2010**, *43*, 137.
[15] Q. Hao, X. Xie, W. Lei, M. Xia, F. Wang, X. Wang, *J. Phys. Chem. C* **2010**, *114*, 9608.
[16] T. Qin, G. Zhou, H. Scheiber, R. E. Bauer, M. Baumgarten, C. E. Anson, E. J. W. List, K. Müllen, *Angew. Chem.* **2008**, *120*, 8416; *Angew. Chem. Int. Ed.* **2008**, *47*, 8292.
[17] T. Qin, W. Wiedemair, S. Nau, R. Trattnig, S. Sax, S. Winkler, A. Vollmer, N. Koch, M. Baumgarten, E. J. W. List, K. Müllen, *J. Am. Chem. Soc.* **2011**, *133*, 1301–1303.
[18] M. D. McKenna, J. Barberá, M. Marcos, J. L. Serrano, *J. Am. Chem. Soc.* **2005**, *127*, 619.
[19] M. Bagui, J. S. Melinger, S. Chakraborty, J. A. Keightley, Z. Peng, *Tetrahedron* **2009**, *65*, 1247.
[20] J. H. Wendorff, T. Christ, B. Glüsen, A. Greiner, A. Kettner, R. Sander, V. Stümpflen, V. V. Tsukruk, *Adv. Mater.* **1997**, *9*, 48.
[21] I. Seguy, P. Destruel, H. Bock, *Synth. Met.* **2000**, *111–112*, 15.
[22] R. Freudenmann, B. Behnisch, M. Hanack, *J. Mater. Chem.* **2001**, *11*, 1618.
[23] B. N. Boden, A. Abdolmaleki, C. T. Z. Ma, M. J. MacLachlan, *Can. J. Chem.* **2008**, *86*, 50.
[24] D. Wang, J. F. Hsu, M. Bagui, V. Dusevich, Y. Wang, Y. Liu, A. J. Holder, Z. Peng, *Tetrahedron Lett.* **2009**, *50*, 2147.
[25] J. Li, Z. He, H. Gopee, A. N. Cammidge, *Org. Lett.* **2010**, *12*, 472.
[26] M. Kaller, C. Deck, A. Meister, G. Hause, A. Baro, S. Laschat, *Chem. Eur. J.* **2010**, *16*, 6326.
[27] J. Miao, L. Zhu, *Soft Matter* **2010**, *6*, 2072.
[28] L. Zhang, H. Gopee, D. L. Hughes, A. N. Cammidge, *Chem. Commun.* **2010**, *46*, 4255.
[29] W. R. Dawson, M. W. Windsor, *J. Phys. Chem.* **1968**, *72*, 3251.
[30] D. Markovitsi, A. Germain, P. Millie, P. Lecuyer, L. Gallos, P. Argyrakis, H. Bengs, H. Ringsdorf, *J. Phys. Chem.* **1995**, *99*, 1005.
[31] J. A. Rego, S. Kumar, H. Ringsdorf, *Chem. Mater.* **1996**, *8*, 1402.

[32] J. W. Levell, A. Ruseckas, J. B. Henry, Y. Wang, A. D. Stretton, A. R. Mount, T. H. Galow, I. D. W. Samuel, *J. Phys. Chem. A* **2010**, *114*, 13291.
[33] D. Zhao, J. S. Moore, *Chem. Commun.* **2003**, 807.
[34] W. Zhang, J. S. Moore, *Angew. Chem.* **2006**, *118*, 4524; *Angew. Chem. Int. Ed.* **2006**, *45*, 4416.
[35] C. Grave, A. D. Schlüter, *Eur. J. Org. Chem.* **2002**, *18*, 3075.
[36] S. Höger, *Chem. Eur. J.* **2004**, *10*, 1320.
[37] H. Bräunling, F. Binnig, H. A. Staab, *Chem. Ber.* **1967**, *100*, 880.
[38] H. Meyer, H. A. Staab, *Liebigs Ann. Chem.* **1969**, *724*, 30.
[39] H. A. Staab, H. Bräunling, *Tetrahedron Lett.* **1965**, *6*, 45.
[40] H. A. Staab, U. E. Meissner, B. Meissner, *Chem. Ber.* **1976**, *109*, 3875.
[41] M. J. Rahman, J. Yamakawa, A. Matsumoto, H. Enozawa, T. Nishinaga, K. Kamada, M. Iyoda, *J. Org. Chem.* **2008**, *73*, 5542.
[42] W. Pisula, M. Kastler, C. Yang, V. Enkelmann, K. Müllen, *Chem. Asian J.* **2007**, *2*, 51.
[43] J. Zhang, X. Wang, Q. Su, L. Zhi, A. Thomas, X. Feng, D. S. Su, R. Schlögl, K. Müllen, *J. Am. Chem. Soc.* **2009**, *131*, 11296.
[44] C. D. Simpson, J. Wu, M. D. Watson, K. Müllen, *J. Mater. Chem.* **2004**, *14*, 494.
[45] W. Pisula, Z. Tomovic, C. Simpson, M. Kastler, T. Pakula, K. Müllen, *Chem. Mater.* **2005**, *17*, 4296.
[46] W. Pisula, A. Menon, M. Stepputat, I. Lieberwirth, U. Kolb, A. Tracz, H. Sirringhaus, T. Pakula, K. Müllen, *Adv. Mater.* **2005**, *17*, 684.
[47] Y.-Z. Lee, X. Chen, S.-A. Chen, P.-K. Wei, W.-S. Fann, *J. Am. Chem. Soc.* **2001**, *123*, 2296.
[48] H.-H. Sung, H.-C. Lin, *Macromolecules* **2004**, *37*, 7945.
[49] Z. Li, M. Lieberman, *Inorg. Chem.* **2001**, *40*, 932.
[50] H. Meier, B. Rose, *J. Prakt. Chem.* **1998**, *340*, 536.
[51] M. V. Bhatt, *Tetrahedron* **1964**, *20*, 803.
[52] T. Yamamoto, *Prog. Polym. Sci.* **1992**, *17*, 1153.
[53] T. Yamamoto, *Bull. Chem. Soc. Jpn.* **1999**, *72*, 621.
[54] R. B. Martin, *Chem. Rev.* **1996**, *96*, 3043.
[55] J. Wu, A. Fechtenkötter, J. Gauss, M. D. Watson, M. Kastler, C. Fechtenkötter, M. Wagner, K. Müllen, *J. Am. Chem. Soc.* **2004**, *126*, 11311.
[56] R. S. Becker, I. S. Singh, E. A. Jackson, *J. Chem. Phys.* **1963**, *38*, 2144.
[57] A. Kreyes, M. Amirkhani, I. Lieberwirth, R. Mauer, F. Laquai, K. Landfester, U. Ziener, *Chem. Mater.* **2010**, *22*, 6453.
[58] Gaussian 03, Revision B.04, M. J. Frisch, G. W. Trucks, H. B. Schlegel, G. E. Scuseria, M. A. Robb, J. R. Cheeseman, J. A. Montgomery, Jr., T. Vreven, K. N. Kudin, J. C. Burant, J. M. Millam, S. S. Iyengar, J. Tomasi, V. Barone, B. Mennucci, M. Cossi, G. Scalmani, N. Rega, G. A. Petersson, H. Nakatsuji, M. Hada, M. Ehara, K. Toyota, R. Fukuda, J. Hasegawa, M. Ishida, T. Nakajima, Y. Honda, O. Kitao, H. Nakai, M. Klene, X. Li, J. E. Knox, H. P. Hratchian, J. B. Cross, V. Bakken, C. Adamo, J. Jaramillo, R. Gomperts, R. E. Stratmann, O. Yazyev, A. J. Austin, R. Cammi, C. Pomelli, J. W. Ochterski, P. Y. Ayala, K. Morokuma, G. A. Voth, P. Salvador, J. J. Dannenberg, V. G. Zakrzewski, S. Dapprich, A. D. Daniels, M. C. Strain, O. Farkas, D. K. Malick, A. D. Rabuck, K. Raghavachari, J. B. Foresman, J. V. Ortiz, Q. Cui, A. G. Baboul, S. Clifford, J. Cioslowski, B. B. Stefanov, G. Liu, A. Liashenko, P. Piskorz, I. Komaromi, R. L. Martin, D. J. Fox, T. Keith, M. A. Al-Laham, C. Y. Peng, A. Nanayakkara, M. Challacombe, P. M. W. Gill, B. Johnson, W. Chen, M. W. Wong, C. Gonzalez, J. A. Pople, Gaussian, Inc., Wallingford CT, **2004**.

Received: March 13, 2011
Published online: July 14, 2011

